Molecular Therapy
Original Article

Orally Targeted Delivery of Tripeptide KPV via Hyaluronic Acid-Functionalized Nanoparticles Efficiently Alleviates Ulcerative Colitis

Bo Xiao,[1,2] Zhigang Xu,[1] Emilie Viennois,[2] Yuchen Zhang,[2] Zhan Zhang,[2] Mingzhen Zhang,[2] Moon Kwon Han,[2] Yuejun Kang,[1] and Didier Merlin[2,3]

[1]Institute for Clean Energy and Advanced Materials, Faculty of Materials and Energy, Southwest University, Chongqing 400715, People's Republic of China; [2]Institute for Biomedical Sciences, Center for Diagnostics and Therapeutics, Georgia State University, Atlanta, GA 30302, USA; [3]Atlanta Veterans Affairs Medical Center, Decatur, GA 30033, USA

Overcoming adverse effects and selectively delivering drug to target cells are two major challenges in the treatment of ulcerative colitis (UC). Lysine-proline-valine (KPV), a naturally occurring tripeptide, has been shown to attenuate the inflammatory responses of colonic cells. Here, we loaded KPV into hyaluronic acid (HA)-functionalized polymeric nanoparticles (NPs). The resultant HA-KPV-NPs had a desirable particle size (~272.3 nm) and a slightly negative zeta potential (~−5.3 mV). These NPs successfully mediated the targeted delivery of KPV to key UC therapy-related cells (colonic epithelial cells and macrophages). In addition, these KPV-loaded NPs appear to be nontoxic and biocompatible with intestinal cells. Intriguingly, we found that HA-KPV-NPs exert combined effects against UC by both accelerating mucosal healing and alleviating inflammation. Oral administration of HA-KPV-NPs encapsulated in a hydrogel (chitosan/alginate) exhibited a much stronger capacity to prevent mucosa damage and downregulate TNF-α, thus they showed a much better therapeutic efficacy against UC in a mouse model, compared with a KPV-NP/hydrogel system. These results collectively demonstrate that our HA-KPV-NP/hydrogel system has the capacity to release HA-KPV-NPs in the colonic lumen and that these NPs subsequently penetrate into colitis tissues and enable KPV to be internalized into target cells, thereby alleviating UC.

INTRODUCTION

Ulcerative colitis (UC) is a chronic, relapsing inflammatory disease in the colon.[1] During the disease formation, inflammation impairs the colonic mucosal barrier, increasing the permeability of epithelial barrier and the chance of bacteria invasion into underlying tissues. This triggers an excessive immune reaction that is believed to induce UC.[2] Thus, the primary goals for clinical UC therapy are to accelerate mucosal healing and alleviate inflammation.[3,4] Current therapeutic strategies are confined to anti-inflammatory agents and immunosuppressive drugs. Although some of these agents can control inflammation, their clinical applications are associated with serious adverse effects such as osteoporosis and increased susceptibility to infection.[5,6] In addition, the currently available drug delivery systems (DDSs) are not very efficient for selective UC therapy.[7] To overcome the risk of drug-related adverse effect and enhance therapeutic efficacy, we urgently need to develop novel therapeutic strategies.

α-Melanocyte-stimulating hormone (α-MSH), an endogenous tridecapeptide, is a cleavage product of proopiomelanocortin that has protective and anti-inflammatory effects.[8,9] Its anti-inflammatory activity has been shown to be mediated by three N-terminal amino acids, lysine-proline-valine (KPV). Interestingly, the KPV peptide was found to exert an even stronger anti-inflammatory effect than α-MSH,[9,10] and we recently demonstrated that KPV could attenuate the inflammatory responses of colonic epithelial and immune cells and reduce the incidence of colitis in vivo upon oral administration.[11,12] We also showed that KPV exerts its anti-inflammatory function inside cells, where it inactivates inflammatory pathways.[12] Moreover, unlike the drugs currently used for UC therapy, KPV is a naturally derived tripeptide without any notable side effects.

At present, nanoparticle (NP)-based DDSs have attracted extensive attention in UC therapy. For example, studies have shown that NPs after oral administration preferentially penetrate throughout the intestinal mucosa and accumulate in colitis tissues, thereby avoiding rapid elimination by diarrhea.[11,13–17] This enhanced accumulation, which might be ascribed to the disordered nature of the mucosal barrier under UC, the impairment of epithelial tight junctions, and/or the immigration of immune cells,[1] has been called the "epithelial enhanced permeability and retention" (eEPR) effect.[18] However, although NPs appear to offer the ability to passively target drugs to colitis tissue, thereby maximizing local drug concentrations, the therapeutic efficacy of passive colitis-targeting NPs is still far from satisfaction.

Received 24 May 2016; accepted 27 November 2016;
http://dx.doi.org/10.1016/j.ymthe.2016.11.020.

Correspondence: Bo Xiao, Institute for Clean Energy and Advanced Materials, Faculty of Materials and Energy, Southwest University, Chongqing 400715, People's Republic of China.
E-mail: bxiao@gsu.edu

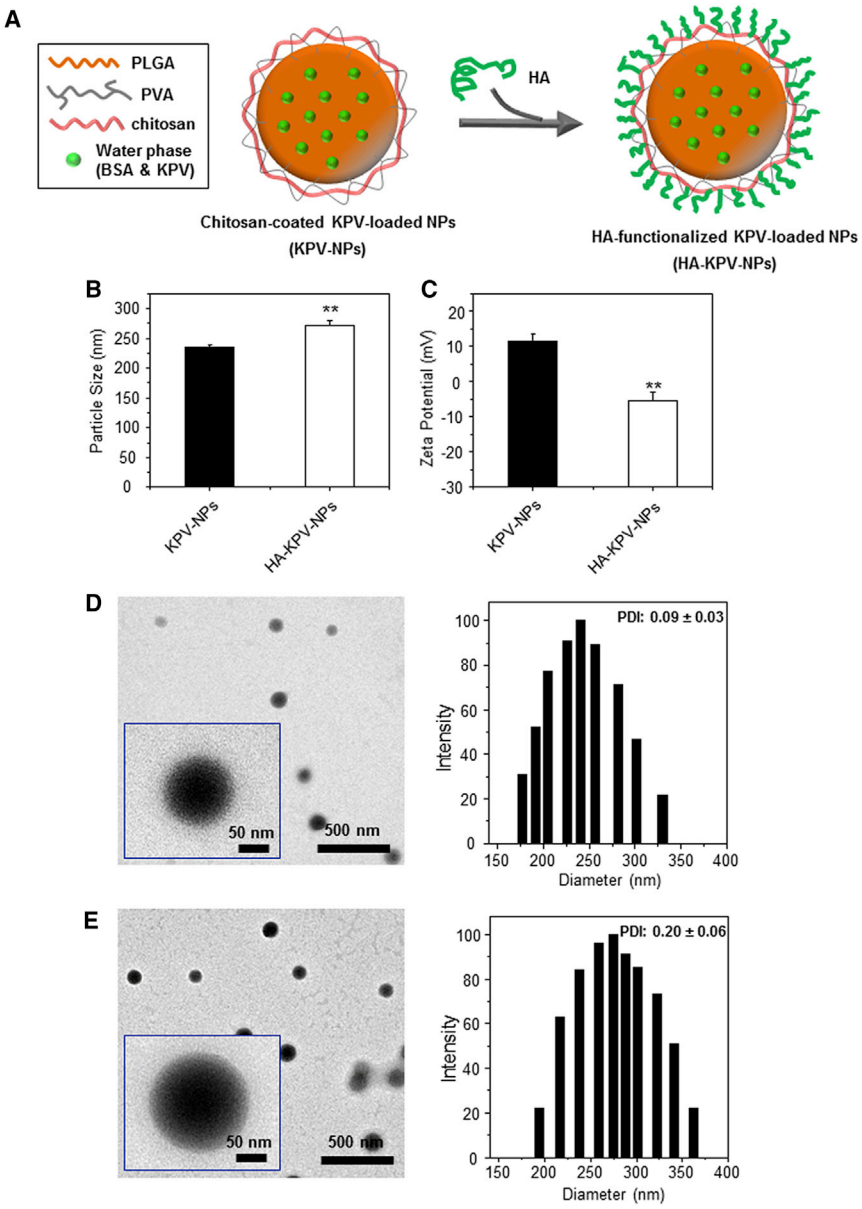

Figure 1. Preparation and Characterization of KPV-Loaded Polymeric NPs

(A) Schematic illustration of the fabrication process of HA-KPV-NPs. (B and C) Particle size (B) and zeta potential (C) of NPs. Data are presented as means ± SEM (n = 3). (D and E) Representative TEM images and the corresponding size distribution of KPV-NPs (D) and HA-KPV-NPs (E). **p < 0.01.

Researchers have sought to improve the cell specificity and cellular uptake efficiency of NPs by modifying their surfaces with targeting ligands that can promote drug accumulation at colitis sites and support efficient internalization of drug by target cells.[19] Ligand-mediated active colitis-targeting modalities have become an emerging approach for efficient UC therapy. Colonic epithelial cells and macrophages, which are closely involved in the inflammatory process of colitis, are considered to be attractive target cells. CD44, a transmembrane glycoprotein and specific receptor for hyaluronic acid (HA), is highly overexpressed on the surface of colonic epithelial cells and macrophages in colitis tissues.[20–22] Thus, it could be an attractive receptor for targeted drug delivery in UC therapy. HA is a natural biocompatible polysaccharide whose functionalization could significantly increase the cellular uptake of NPs via HA receptor-mediated endocytosis.[23,24] Poly(lactic acid/glycolic acid) (PLGA), an FDA-approved biodegradable polymer, can efficiently encapsulate hydrophilic factors (e.g., plasmids, small interfering RNAs [siRNAs], and proteins)[25–27] and thus have been recognized as an attractive material for drug delivery.

Here, we fabricated HA-functionalized KPV-loaded PLGA NPs (HA-KPV-NPs; depicted in Figure 1A), characterized their physicochemical properties (e.g., hydrodynamic particle size, zeta potential, drug loading, morphology), and further examined their targeted drug delivery profiles. Moreover, we investigated their abilities to accelerate mucosal healing and alleviate inflammation in vitro and in a dextran sulfate sodium (DSS)-induced UC mouse model.

RESULTS

Fabrication of NPs

KPV-loaded NPs were fabricated using a water-in-oil-in-water (W/O/W) double emulsion-solvent evaporation method, which is a well-established technique for preparing hydrophilic agent-loaded polymeric NPs.[28] Briefly, the inner aqueous phase (KPV/BSA) was mixed with the organic phase (PLGA) to form a first W/O emulsion under sonication. This first emulsion was sonicated with the second aqueous phase (poly [vinyl alcohol] [PVA] and chitosan)We to form a W/O/W emulsion based on the Gibbs-Marangoni effect.[29] As the organic solvent (dichloromethane) evaporated, the inner aqueous phase (KPV/BSA) was efficiently restricted into the hydrophobic PLGA core. PVA is a common amphiphilic polymer that is widely used as an emulsifier for the preparation of polyester NPs.[30] The addition of PVA to the second aqueous phase resulted in the partitioning of its hydrophobic segments into the hydrophobic PLGA matrix and the outward display of its hydrophilic segments, thereby stabilizing the NPs.[31] We have often used amino group-bearing chitosan for the further surface modification of PLGA NPs,[23,32,33] whereby chitosan likely entangles its molecular chains with PVA and/or adsorbs to the negatively charged NP surface. Finally, HA was conjugated to the

chitosan-modified NPs via the formation of an amide bond between the amino group of chitosan and the carboxyl group of HA, using 1-ethyl-3-(3-dimethylaminopropyl)-carbodiimide (EDC)/*N*-hydroxysuccinimide (NHS) chemistry in 2-(*N*-morpholino) ethanesulfonic acid sodium salt (MES) buffer. On the basis of this strategy, we obtained the desired HA-functionalized NPs (Figure 1A).

Physicochemical Characterization of NPs

Particle size and zeta potential are important parameters that directly impact the stability, bio-distribution, and cellular uptake profiles of NPs.[29] These parameters were measured in acidic solution, and the pH value (6.2) was selected because it represented the physiological pH condition in the colonic lumen. As shown in Figure 1B, dynamic light scattering (DLS) measurements revealed that the average hydrodynamic diameter of KPV-NPs was about 235.2 nm, whereas that of HA-KPV-NPs was 272.3 nm. As shown in Figure 1C, KPV-NPs were found to be electropositive, whereas HA-KPV-NPs exhibited a negative zeta potential at about −5.3 mV, reflecting the successful conjugation of negatively charged HA to the NP surface. The NP morphology was examined by transmission electron microscopy (TEM). As seen in representative TEM images, KPV-NPs (Figure 1D) and HA-KPV-NPs (Figure 1E) were spherical in shape with mean diameters less than 160 nm and exhibited narrow size distributions. The discrepancies in the diameters measured by DLS and TEM may be attributed to the differences in the NP surface states under the test conditions. As described in our previous study,[33] NPs are in a swollen state when examined by DLS, whereas they must be fully dehydrated for TEM characterization. As reported, cells tend to internalize NPs with diameters less than 400 nm;[34,35] NPs with diameters less than 10 μm preferentially accumulate in colitis tissues based on the eEPR effect; and inflamed mucosa exhibits accumulation of positively charged proteins.[36] Therefore, the properties of our HA-KPV-NPs should favor their penetration into inflamed colon tissue, adhesion to the positively charged inflamed mucosa, and further internalization into target cells.

The hexadecyltrimethylammonium bromide turbidimetric method (CTM) has been demonstrated as an accurate, sensitive and specific method for HA quantification.[37,38] Thus, it was applied to quantify HA amount on the surface of HA-KPV-NPs in the present study. We found that the HA amount on HA-KPV-NPs was 63.1 ± 1.4 μg/mg of NPs. The KPV encapsulation rate of NPs was calculated as described in our previous report.[11] The encapsulation rates observed for KPV-NPs and HA-KPV-NPs were 52.3 ± 4.2% and 39.7 ± 3.6%, respectively. The ratios of the loaded KPV concentrations versus the dry weights of NPs were 64.3 ± 1.4 and 45.7 ± 2.1 ng/mg, respectively. It was found that the encapsulation rate and KPV loading amount of HA-KPV-NPs were much lower than that of KPV-NPs, which might be due to the release of KPV near the NP surface to the reaction solution during the process of HA conjugation.

Cytotoxicity of HA-KPV-NPs

To evaluate the cytotoxicity of the developed NPs, we performed in vitro cytotoxicity tests of KPV-NPs and HA-KPV-NPs against Colon-26 cells and Raw 264.7 macrophages. The results from 3-(4,5-dimethylthiazol-2-yl)-2,5-diphenyl tetrazolium bromide (MTT) assays (Figure S1) revealed no obvious cytotoxicity in either cell line following incubation with KPV-NPs or HA-KPV-NPs, even after 48 hr. This indicates that the generated NPs have excellent biocompatibility.

Cellular Uptake of HA-Functionalized NPs

Because KPV functions inside cells,[12] efficient cellular uptake is a major requirement for the therapeutic efficacy of KPV-loaded NPs. To track the HA-functionalized NPs in cells, we used coumarin-6 (CM) as a fluorescent probe. HA-CM-NPs were fabricated using an oil-in-water (O/W) emulsion-solvent evaporation method, as described in our previous report.[33] The amount of CM in HA-CM-NPs was examined by measuring its intrinsic fluorescence. To investigate the internalization profiles of the NPs in two cell types that are believed to be key UC therapy-related cells, we co-incubated Colon-26 cells and Raw 264.7 macrophages with HA-CM-NPs (CM, 50 μM) for 5 hr. As expected, clear drug accumulation was detected in both cell lines after treatment with HA-CM-NPs (Figure 2A), whereas untreated control cells showed no fluorescence (data not shown).

We next evaluated the tissue uptake profile of HA-functionalized NPs by colitis tissue. As shown in Figure 2B, tissue sections revealed abundant internalization of HA-CM-NPs (green) into colonic epithelial cells after 5 hr of co-incubation. Critically, many NPs penetrated deeply into the inflamed tissue.

To quantitatively compare the cellular uptake efficiency of non-functionalized NPs and HA-functionalized NPs, we treated Colon-26 cells and Raw 264.7 macrophages with CM-NPs or HA-CM-NPs and used flow cytometry (FCM) to investigate their cellular uptake profiles after 0, 1, 3, and 5 hr of co-incubation. As shown in Figure 3, the fluorescence intensities were markedly higher in the HA-CM-NP-treated cell lines compared with the corresponding CM-NP-treated cells. This indicates that surface functionalization with HA can promote the cellular uptake efficiency of NPs by target cells.

Promotion of Mucosal Healing by HA-KPV-NPs

Enhancement of mucosal healing is one of the two major aims in UC treatment.[18] Because KPV was shown to decrease the inflammatory response of colonic epithelial cells to inflammatory stimulation,[12] it was reasonable to speculate that HA-KPV-NPs might be able to improve the healing of an inflamed mucosal layer. Thus, we investigated the effects of HA-KPV-NPs on wound healing using electrical impedance sensing (ECIS) technology. Caco2-BBE monolayers grown on ECIS 8W1E plates were wounded with a 30 s electrical pulse (frequency 40 kHz, amplitude 4.5 V). As shown in Figure 4, wounded epithelial layers treated with HA-KPV-NP suspensions showed significant and dose-dependent increases in recovery, compared with untreated control layers. These results clearly demonstrate that HA-KPV-NPs can enhance the healing of a wounded colonic epithelial layer.

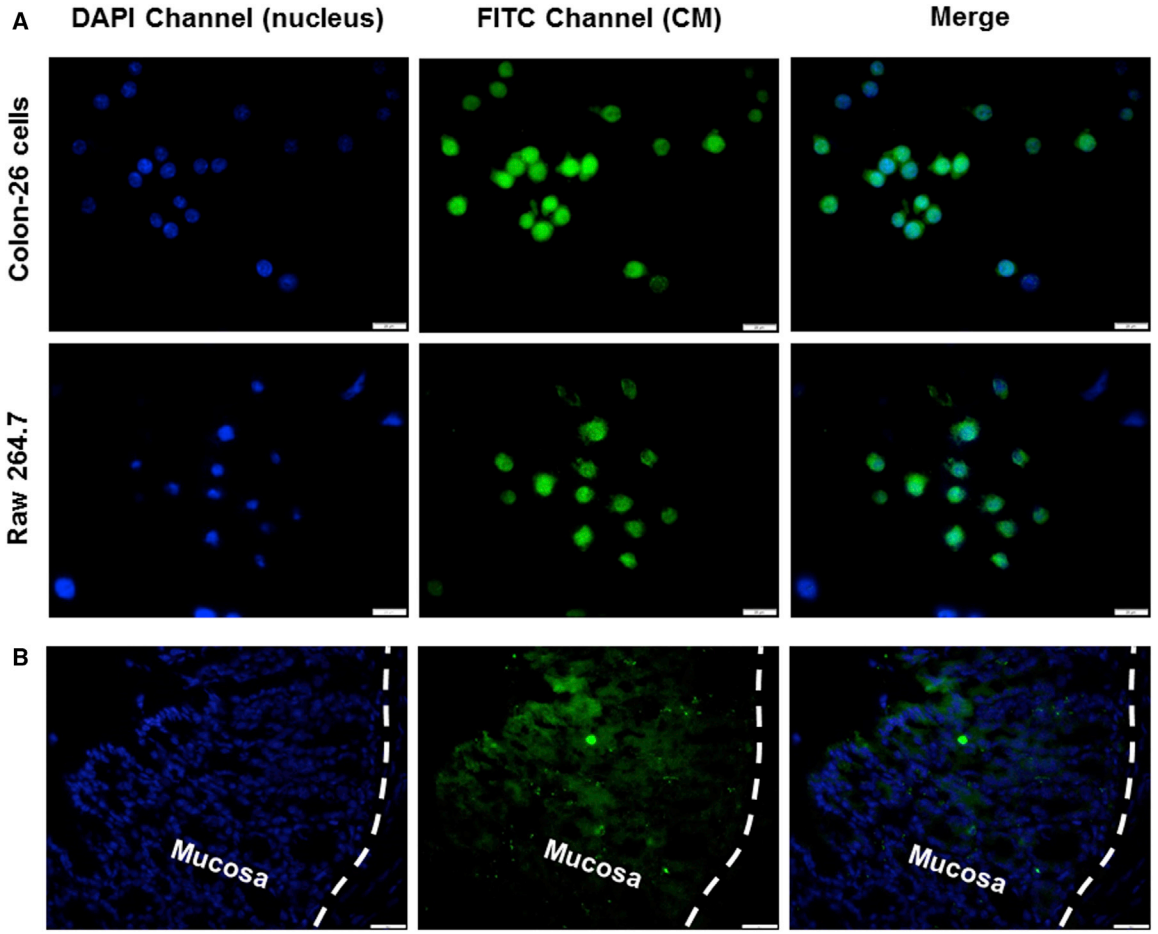

Figure 2. Uptake Profiles of HA-CM-NPs by Colon-26 Cells, Raw 264.7 Macrophages, and Colitis Tissue

(A) Cellular uptake of HA-CM-NPs (green) by respective Colon-26 cells and Raw 264.7 macrophages. Cells were treated with NPs (CM, 50 μM) for 5 hr and processed for fluorescence staining. Fixed cells were stained with DAPI for visualization of nuclei (purple). The scale bars represent 10 μm. (B) Colitis tissue uptake of NPs after 5 hr of co-incubation. Colitis tissue were treated with NPs (CM, 100 μM), sectioned and processed for fluorescence staining. Fixed tissues were stained with DAPI for visualization of nuclei (purple). The scale bars represent 50 μm.

Reduced TNF-α mRNA Expression Level In Vitro by HA-KPV-NPs

The in vitro anti-inflammatory properties of KPV-loaded NPs were assessed using qRT-PCR. We treated Raw 264.7 macrophages with NPs and assessed the TNF-α mRNA expression level, which is a crucial factor that is mainly secreted by macrophages during the onset and progression of UC.[6] As shown in Figure 5, untreated Raw 264.7 macrophages treated with lipopolysaccharide (LPS, 1 μg/mL; to stimulate an inflammatory response) exhibited marked increases of TNF-α mRNA expression level after 24 and 48 hr. In contrast, this effect was considerably reduced in cells pre-treated with KPV-loaded NPs. We further found that LPS-treated Raw 264.7 macrophages pre-treated with HA-KPV-NPs maintained their decreased levels of TNF-α even at 72 and 96 hr post-treatment (Figure S2). Furthermore, cells treated with HA-KPV-NPs had significantly lower TNF-α mRNA expression levels compared with those treated with KPV-NPs. These results, which were consistent with the results of FCM-based in vitro cellular uptake studies (Figure 3), might reflect the enhanced intracellular uptake of HA-KPV-NPs by rapid CD44 receptor-mediated endocytosis.

Enhanced Tissue/Cellular Uptake of Orally Administered HA-Functionalized NPs In Vivo

The DSS-induced UC mouse model is an easily generated and highly reproducible model that resembles human UC.[39,40] To enable NPs to be delivered to the colonic lumen, we encapsulated them in a hydrogel of alginate and chitosan (weight ratio 7:3). The double-gavage protocol can be found at the following link: http://www.nature.com/protocolexchange/protocols/588. We previously reported that this hydrogel collapsed at colonic pH,[11,41] suggesting that NPs should be primarily released to the colonic lumen rather than other sections of gastrointestinal tract (GIT).

To investigate the in vivo bio-distribution of HA-functionalized NPs in GIT, we orally administered DSS-treated mice (a model of UC)

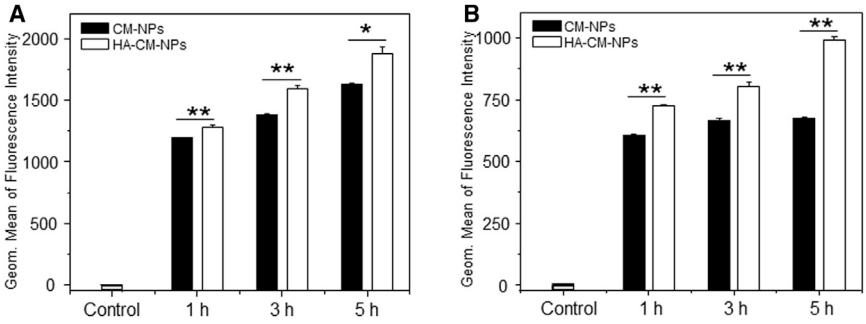

Figure 3. HA Functionalization Increases the Cellular Uptake of NPs by Colon-26 Cells and Raw 264.7 Macrophages

(A and B) Quantification of CM fluorescent intensity in Colon-26 cells (A) and Raw 267.4 macrophages (B) after treatment with respective CM concentrations of 25 and 50 μM. Each point represents the mean ± SEM (n = 3). Statistical significance was assessed using Student's t test (*$p < 0.05$ and **$p < 0.01$).

with DiR-loaded NPs encapsulated in hydrogel, and examined the time-dependent passage and in vivo targeting efficacy of the formulations using near infrared fluorescence (NIRF) imaging. As shown in Figure 6A, a strong NIRF signal was observed in the small intestine at 4 hr after oral administration. Furthermore, we found that HA-DiR-NP-treated mice exhibited significantly stronger fluorescence intensity in colon than DiR-NP-treated mice after 4 hr of oral administration (Figure 6B). A similar trend was also observed after 18 hr. In addition, the fluorescence in colon was hardly detected by 24 hr post-administration (data not shown), and thus mice were gavaged daily during the treatment.

To examine the percentage of macrophages in colitis tissue that internalized HA-functionalized NPs, we gavaged DSS-treated mice with hydrogel containing HA-CM-NPs and carried out FCM analysis. A 5 mg/kg dose of CM was chosen for this experiment. It was reported that macrophages were traditionally considered as part of a linear mononuclear phagocytic system and exclusively derived from blood monocytes.[42] Previous reports showed that monocytes can give rise to intestinal macrophages during inflammation in both humans and mice,[43,44] and more recent research has indicated that macrophages come from two sources: embryonic precursors (characterized as $CD11b^{+}F4/80^{hi}$ cells) and conventional hematopoiesis ($CD11b^{+}F4/80^{lo}$ cells).[45] Figure S3 shows the analytic process of both macrophage sources. As seen in Figure 6C, the percentages of $CD11b^{+}F4/80^{lo}$ colonic macrophages and $CD11b^{+}F4/80^{hi}$ macrophages that had taken up HA-CM-NPs by 12 hr post-administration were 74.7% and 10.4%, respectively. However, for CM-NP-treated mice, these percentages decreased to 66.1% and 4.8%, respectively. This confirmed the targeting capability of the surface-conjugated HA groups in vivo and was consistent with the in vitro results (Figure 2B).

Promoted Therapeutic Efficacy against UC with Orally Administered HA-KPV-NPs

In the present study, we examined whether oral administration of HA-KPV-NPs had a better therapeutic efficacy in relieving UC than orally administrated KPV-NPs. Initially, we evaluated body weight loss, which is a main indicator of the colitis phenotype, among groups of mice subjected to oral administration of hydrogel loaded with different NPs. As shown in Figure 7A, the body weight losses peaked on days 14, 12, and 11 post-treatment for DSS control, KPV-NP-treated and HA-KPV-NP-treated mice, respectively. The HA-KPV-NP-treated mice showed the smallest maximal loss of body weight, and thereafter exhibited the best body weight recovery among the three DSS-treated groups.

Myeloperoxidase (MPO) is an endogenous enzyme of mammalian granulocytes that plays a vital role in the development of UC.[13] Here, MPO activity was used as a direct indicator of the infiltration of granulocytes into colonic mucosa. As shown in Figure 7B, the colonic MPO activity of the DSS-treated control group was significantly higher than that of the healthy control group. In contrast, mice treated with KPV-NPs or HA-KPV-NPs did not show marked differences in MPO activity compared with healthy control mice. The MPO activity of HA-KPV-NP-treated mice was much lower (though not to a significant degree) than that of KPV-NP-treated mice.

In the context of other parameters, DSS-treated control and KPV-NP-treated mice had significantly higher spleen weights compared with the healthy control group, whereas that of the HA-KPV-NP-treated group did not significantly differ versus the healthy control group (Figure 7C). The colon lengths of different groups exhibited a pattern similar to that of spleen weight (Figure 7D). In terms of TNF-α mRNA expression level (Figure 7E), the DSS-treated control group showed the highest expression level; the KPV-NP-treated group showed a lower expression level that was still significantly higher than that of the healthy control group; and there was no marked difference between HA-KPV-NP-treated and healthy control mice.

Colon tissue histology, which is important when investigating the therapeutic efficacy of various treatments, was assessed by H&E staining of colon tissue sections. As shown in Figure 7F, colon tissues from the healthy control group showed no sign of inflammation or disruption of the healthy tissue morphology. In contrast, colon tissues from the DSS-treated control group exhibited clear signs of inflammation, including epithelial disruption, goblet cell depletion, and significant infiltration of inflammatory cells into the mucosa. Interestingly, tissues from the treatment groups showed much less inflammation. Indeed, colon tissues from HA-KPV-NP-treated group were morphologically very similar to those of the healthy control group, especially with respect to the integration of the colonic epithelial layer and the

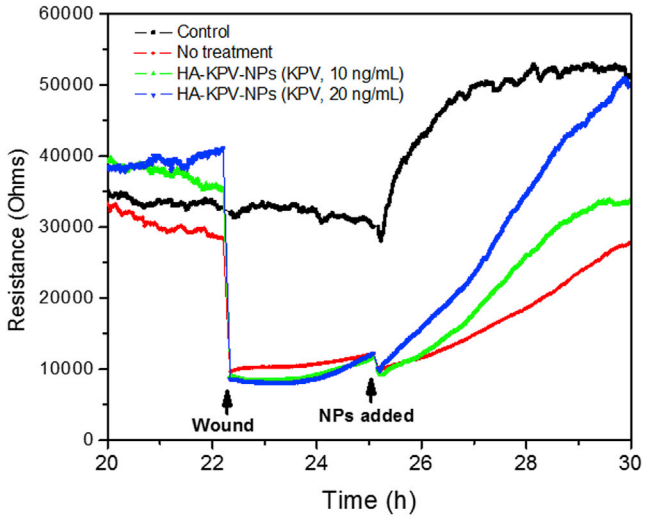

Figure 4. Wound Healing Assay of Caco2-BBE Cells with the Treatment of HA-KPV-NPs on the Basis of the ECIS Technique

The variation of the impedance before and after wounding is shown. One hundred thousand cells per well were seeded into ECIS 8W1E arrays.

infiltration of inflammatory cells. Collectively, our in vitro and in vivo data clearly demonstrate that HA-KPV-NPs show much better therapeutic efficacy than KPV-NPs and can efficiently promote recovery from UC.

DISCUSSION

In the development of novel drug formulations, the goal is to maximize the therapeutic efficacy of the drug while minimizing undesirable adverse effects.[46] To achieve this goal, targeted drug delivery is considered a promising strategy. In the context of delivering UC therapeutics via oral administration, drug delivery can be targeted at the level of the colon (organism level), the inflamed colon sites (tissue level), and the target cells (cell level).[18] Currently, most oral DDSs, such as pellets, capsules, and tablets, are based on pH-, pressure-, time-, or bacteria-responsive mechanisms[47] and can target only the colon. In contrast, NP-based DDSs have the capacity to accumulate in colitis tissues because of the eEPR effect. Lamprecht et al.[48] demonstrated that orally administered NPs tended to accumulate in the inflamed mucosa of rats with colitis. Recently, inflamed colon-targeting DDSs, which rely on the specific features of the inflamed colon, have been developed. As large amounts of positively charged proteins are known to accumulate in inflamed mucosa, Zhang et al.[36] developed a negatively charged hydrogel and demonstrated that the drug-loaded hydrogel preferentially adhered to the inflamed colonic mucosa of mice with UC and human UC patients. In addition, a previous study confirmed that anionic liposomes prefer to attach to the inflamed intestine.[49] It is generally accepted that disintegration of the colonic epithelial layer is strongly linked to mucosal inflammation during the pathogenesis of UC.[18] Therefore, both colonic epithelial cells and macrophages are potential target cells in UC therapy. However, very few target cell-oriented DDSs have been developed to date.

We previously reported that non-functionalized KPV-NPs yielded a therapeutic efficacy similar to that of free KPV solution at a 12,000-fold lower concentration of KPV.[11] Thus, we speculated that the efficiency of this DDS might be increased by endowing with the function of cell specificity. Accordingly, we herein functionalized these NPs with HA, in an effort to enhance the selective delivery of KPV to target cells. To prevent the degradation during transit through the gastrointestinal transit, we encapsulated the NPs into a chitosan/alginate hydrogel. This hydrogel collapses at colonic pH and was used as colon-targeting (organism level) DDS in our previous reports.[11,13–15] Once the negatively charged HA-KPV-NPs are released from the hydrogel, they should accumulate in the positively charged inflamed colonic mucosa and then penetrate through the disrupted epithelial layer into the underlying lamina propria because of the eEPR effect (tissue level; Figure 2B).[19] Finally, the HA-KPV-NPs should be internalized into CD44-overexpressing colonic epithelial cells and macrophages at the inflamed colonic sites (cell level).

Indeed, the results obtained from the in vitro cellular uptake study (Figure 3) supported our hypothesis that compared with KPV-NPs, HA-KPV-NPs allowed increased uptake by colonic epithelial cells and macrophages. HA-KPV-NPs were also found to accelerate mucosal healing and alleviate inflammation (Figures 4 and 5), and their HA functionalization and subsequent increased uptake by target cells were associated with a much higher efficiency in alleviating UC compared to non-functionalized KPV-NPs (Figure 6). In addition, the tested parameters (body weight, MPO activity, colon length, spleen weight, and histologic appearance) were very similar between HA-KPV-NP-treated mice and healthy controls (Figure 7).

Compared with other oral DDSs reported for UC therapy, our HA-KPV-NP-embedded hydrogel system has a number of unique beneficial features. First, it has excellent biocompatibility. KPV is a naturally derived tripeptide without notable toxicity, and all of the carrier materials used are nontoxic and generally recognized as safe (GRAS) polymers, which should facilitate their rapid translation to clinical application. Second, the system has excellent stability. The solid phase of PLGA NPs allows long-term storage and convenient use in the clinic. In addition, they are stable following the release from the hydrogel to the colonic lumen and thus can protect KPV from degradation. Third, it has cell specificity. This oral HA-functionalized NP-hydrogel system appears to target at the colon and inflamed colonic sites and actively target the delivery of KPV to key UC therapy-related cells (colonic epithelial cell and macrophages), as summarized in our proposed model (Figure 8). Fourth, fabrication is easy. The process for preparing this NP-hydrogel system is relatively simple and easy to scale up. Finally, the cost is low. The drug and polymers used in this DDS are relatively inexpensive and available in large quantities.

In conclusion, we report a new strategy that uses a HA-functionalized NP-hydrogel system prepared from GRAS reagents for the targeted delivery of KPV to both epithelial cells and macrophages in colitis tissues. Through its ability to release HA-KPV-NPs to the colonic lumen, attach to inflamed mucosa, and accumulate in target cells,

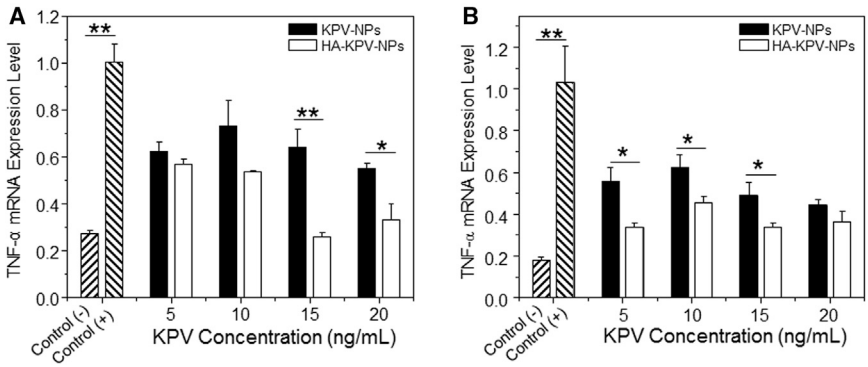

Figure 5. In Vitro TNF-α Gene Downregulation Capacities of KPV-NPs and HA-KPV-NPs against Raw 267.4 Macrophages

In vitro TNF-α gene downregulation capacities of KPV-NPs and HA-KPV-NPs against Raw 267.4 macrophages for 24 hr (A) and 48 hr (B). After treatment by NPs, cells were treated with LPS (1 μg/mL) for 3 hr. Each point represents the mean ± SEM (n = 3). Statistical significance was assessed using the Student's t test (*$p < 0.05$, **$p < 0.01$).

this system has the capacity to promote mucosal healing and decrease inflammation. Thus, HA-KPV-NP-embedded hydrogel may be an attractive therapeutic strategy against UC.

MATERIALS AND METHODS

Materials

PLGA (molecular weight [MW] = 38–54 kg/mol), PVA (86%–89% hydrolyzed, low molecular weight), chitosan, sodium nitrite, CM, EDC, NHS, MES, cetyltrimethylammonium bromide, and LPS from *Salmonella* enteric serotype typhimurium were purchased from Sigma-Aldrich. KPV was purchased from KareBay Biochem. The molecular weight of chitosan was tailored by depolymerization using sodium nitrite following a reported method.[50] Viscosity-average molecular weight of the resulting chitosan was determined as 1.8×10^4 using a reported method.[51] The depolymerized chitosan was used in the NP fabrication process. HA (MW = 20 kDa) was obtained from Lifecore Biomedical. Paraformaldehyde stock solution (16%) was from Electron Microscopy Science. MTT was supplied from Invitrogen. DSS (36–50 kDa) was obtained from MP Biomedicals. Buffered formalin (10%) was supplied from EMD Millipore. H&E were from Richard-Allan Scientific. All commercial products were used without further purification.

Fabrication of HA-KPV-NPs

NPs were prepared by a double emulsion solvent evaporation technique. Briefly, a primary aqueous phase containing BSA (50 mg/mL) and KPV (6 mg/mL) was prepared in water. PLGA (100 mg) was dissolved in 2 mL of dichloromethane. The aqueous solution was then added dropwise to the oil phase to form the first emulsion. Addition of this emulsion to 4 mL PVA solutions (5%) with depolymerized chitosan (0.5%) and subsequent sonication (six times, 10 s each time) of the whole mixture formed a double emulsion. This double emulsion was immediately poured into 100 mL of aqueous solution containing 0.3% PVA with 0.03% depolymerized chitosan. After that, the organic solvent was evaporated under low vacuum conditions (Rotary evaporator, Yamato RE200). The NPs formed by this method were collected by centrifugation at 12,000 × *g* for 20 min and washed three times with deionized water.

As to the fabrication of HA-functionalized NPs, the CS-KPV-NPs obtained above were dispersed in MES buffer (pH 5.5). The carboxyl group of HA was activated for 2 hr by NHS/EDC. The HA solution was added to CS-KPV-NPs suspension, and resultant mixture was allowed to react at ambient temperature with stirring for 4 hr. The final NPs were collected by centrifugation at 12,000 × *g* for 20 min, washed three times with deionized water, dried in a lyophilizer, and stored at −20°C in an airtight container.

Characterization of NPs

Particle sizes (nanometers) and zeta potential (millivolts) of NPs were measured by DLS using 90 Plus/BI-MAS (multi-angle particle sizing) or DLS after applying an electric field using a ZetaPlus (zeta potential analyzer, Brookhaven Instruments). The averages and SDs of the diameters (nanometers) or zeta potential (millivolts) were calculated using three runs. Each run was an average of 10 measurements. The average values were based on the measurement on repeated NPs. The morphology of NPs was observed with a TEM (LEO 906E, Zeiss). A drop of diluted NP suspension was mounted onto 400-mesh carbon-coated copper grids and dried before analysis.

The amount of HA on the surface of HA-KPV-NPs was quantified using the CTM as reported previously.[52,53] Briefly, NPs (5 mg) were dissolved in dichloromethane at room temperature for 15 min. The free HA or HA conjugates were extracted from the organic phase using 0.8 mL sodium acetate solution (0.2 M). Sodium acetate solution was added to the organic solution, and the resultant mixture was vortexed vigorously for 5 min and then centrifuged at 12,000 rpm for 5 min at 4°C. The HA content in the supernatant was further analyzed. Fifty microliters of HA standard solution (0.05–2 mg/mL) or HA sample was added to a 96-well plate. The solutions were incubated with 50 μL of sodium acetate solution (0.2 M) for 10 min at 37°C. Then, 100 μL of 10 mM cetyltrimethylammonium bromide solution was added to the mixture, and the absorbance of the precipitated complex was read after 10 min of co-incubation against the blank at 570 nm using a microplate reader. The amount of HA to HA-KPV-NPs was then calculated by previously drawn standard curve of native HA.

The loading amount of KPV in NPs was determined using our previous method.[11] NPs (3 mg) were vortexed in 0.5 mL of dichloromethane. The released BSA/KPV was extracted from the organic phase using 0.8 mL PBS. PBS was added to the organic solution, and the

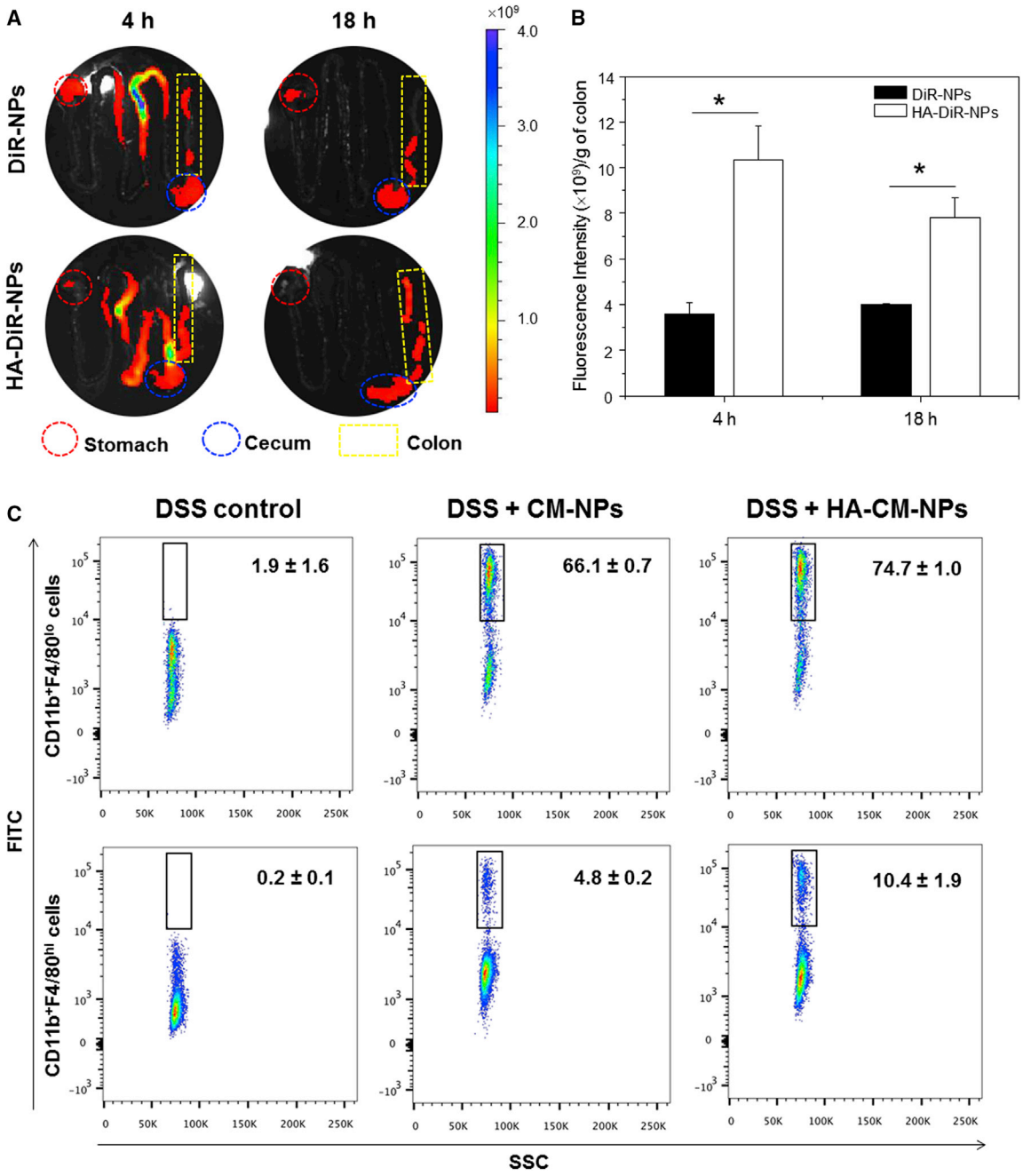

Figure 6. HA Functionalization Increases the Tissue/Cellular Uptake of NPs after Oral Administration in Mice with Colitis

(A) Typical images of GIT imaging showing accumulation of orally NPs embedded in hydrogel in colon at different time points (4 and 18 hr). (B) Quantification of the fluorescence intensity in colon tissue. (C) Representative FCM analysis of CM fluorescence-positive macrophages in mice receiving DSS and treated with hydrogel with CM-NPs or HA-CM-NPs. Data are expressed as mean ± SEM (n = 3). *p < 0.05.

resultant mixture was vortexed vigorously for 5 min and then centrifuged at 12,000 rpm for 5 min at 4°C. The BSA content in the supernatant was analyzed by the Bio-Rad protein assay. The encapsulation rate was applied to determine the KPV loading, assuming that BSA and KPV are loaded in the same way in a homogeneous aqueous phase.

Biocompatibility of NPs

For MTT assay, Colon-26 cells and Raw 264.7 macrophages were seeded at densities of 2×10^4 and 8×10^3 cells/well, respectively, in 96-well plates and incubated overnight. After 24 or 48 hr of exposure to NP suspensions, the cells were then incubated with MTT reagent

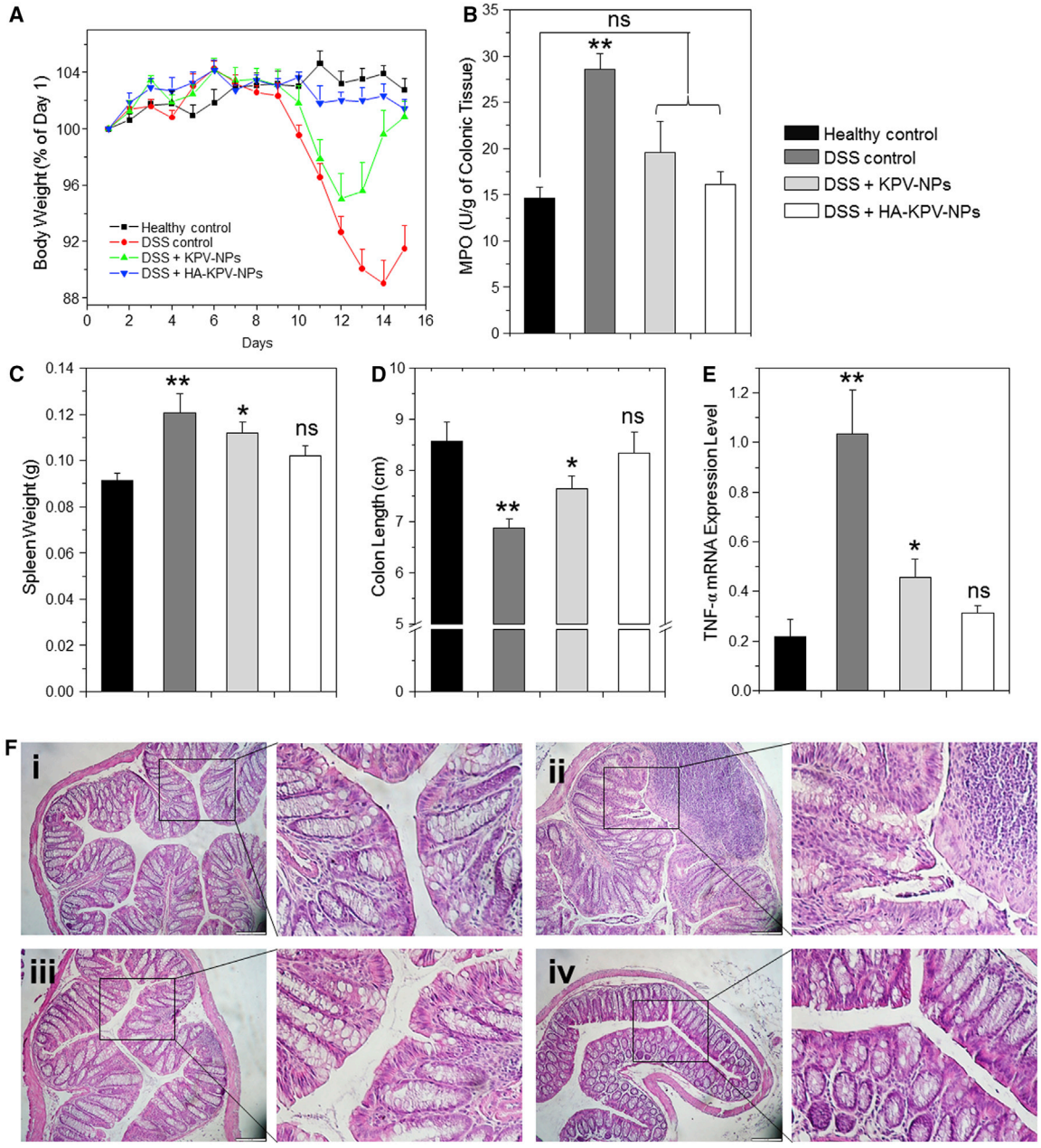

Figure 7. Oral Administration of KPV-NP- or HA-KPV-NP-Embedded Hydrogel Relieve DSS-Induced UC in Mice

(A) Mouse body weight over time, normalized as a percentage of day 1 body weight and given as the mean of each treatment group. (B–E) Colonic MPO activity (B), spleen weight (C), colon length (D), and TNF-α mRNA expression levels (E) in different treatment mice groups. The MPO results are expressed as units of MPO activity per gram of tissue. Each point represents the mean ± SEM (n = 5). Statistical significance was assessed using ANOVA followed by a Bonferroni post-test (*$p < 0.05$, **$p < 0.01$). (F) Representative H&E-stained colon sections from DSS-treated mice administered with daily double gavages of hydrogel with different NPs for 6 days: (i) healthy control mice group, (ii) DSS-treated mice group, (iii) KPV-treated mice group, and (iv) HA-KPV-NP-treated mice group. The scale bars represent 100 μm.

(0.5 mg/mL in supplemented 100 μL of serum-free medium) at 37°C for 4 hr. Thereafter, the media were discarded, and 50 μL DMSO was added to each well prior to spectrophotometric measurements at 570 nm. Untreated cells were used as a negative reference, whereas cells treated with 0.5% Triton X-100 were the positive control.

Intracellular NP Uptake Visualization

To investigate the cellular uptake profiles of the HA-functionalized NPs, CM was used as a fluorescence probe. CM-NPs and HA-CM-NPs were prepared by an oil-in-water emulsion-solvent evaporation technique as we reported previously.[23,32,33] The amount of CM in

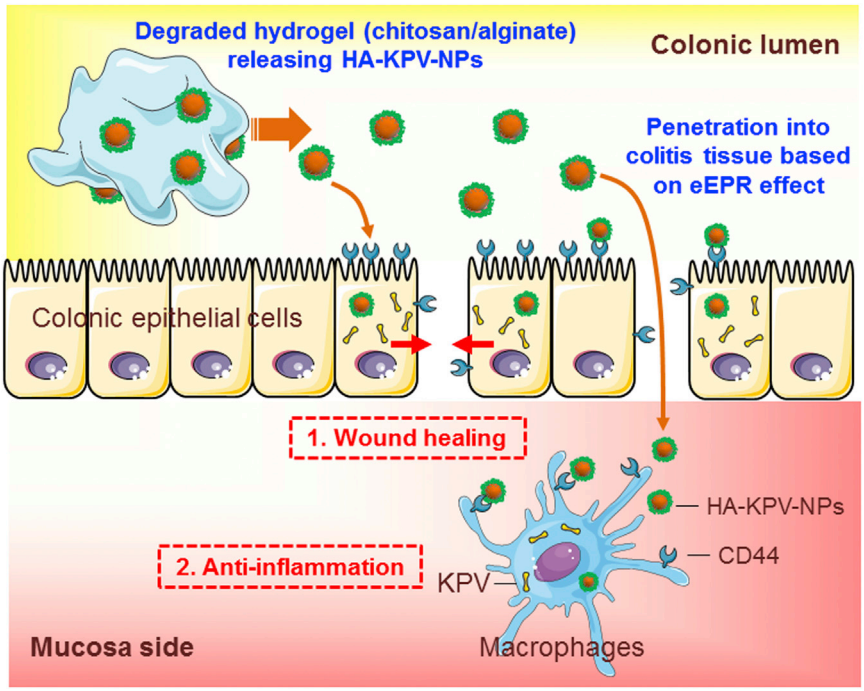

Figure 8. The Therapeutic Effects of HA-KPV-NPs against UC

Oral administration of HA-KPV-NPs embedded in hydrogel (chitosan/alginate) confers combined therapeutic effects against UC by accelerating mucosa healing and alleviating inflammation.

the NPs was examined by measuring its intrinsic fluorescence on a PerkinElmer EnSpire multimode plate reader (PerkinElmer). Colon-26 cells and Raw 264.7 macrophages were seeded in eight-chamber tissue culture glass slide (BD Falcon) at densities of 5×10^4 and 2×10^4 cells/well, respectively, and incubated overnight. After 5 hr of exposure to HA-CM-NPs (CM, 50 μM), the cells were thoroughly rinsed with PBS to eliminate excess of NPs and then fixed in 4% paraformaldehyde for 20 min. To observe cellular uptake of NPs, DAPI was diluted 10,000 times and added to the wells for staining cells for 5 min. Images were acquired using the fluorescein isothiocyanate (FITC) channel and DAPI channel on an Olympus fluorescence microscopy equipped with a Hamamatsu Digital Camera ORCA-03G.

Quantification of Cellular Uptake Using FCM

Colon-26 cells and Raw 264.7 macrophages were seeded in 12-well plates at densities of 4×10^5 and 1×10^5 cells/well, respectively, and incubated overnight. The medium was exchanged to serum-free medium containing CS-CM-NPs or HA-CM-NPs (equal to 25 and 50 μM CM for Colon-26 cells and Raw 264.7 macrophages, respectively). Cells treated with blank NPs were used as negative controls. After incubation for different time periods (0, 1, 3, and 5 h), the cells were thoroughly rinsed with PBS to eliminate excess NPs, which were not taken up by cells. Subsequently, the treated cells were harvested using Accutase or trypsin, transferred to centrifuge tubes, and centrifuged at 1,500 rpm for 5 min. Upon removal of the supernatant, the cells were re-suspended in FCM buffer, transferred to round-bottom polystyrene test tubes (12 × 75 mm, BD Falcon), and kept at 4°C until further analysis. Analytical FCM was performed using the FITC channel on the FCM Canto (BD Biosciences). A total of 5,000 ungated cells were analyzed.

In Vitro Wound Healing Assay

Wound healing assays were performed using ECIS technology (Applied BioPhysics). The ECIS model 1600R was used for these experiments. The measurement system consists of an eight-well culture dish (ECIS 8W1E plate), the surface of which is seeded with Caco2-BBE cells at a density of 1×10^6/well. Once cells reached confluence, an elevated current pulse (3 mA, 40 kHz, 30 s) was used to wound the confluent cell monolayer. The wounding pulse was reflected by a sharp drop in resistance. The system then switched back to its normal operation to monitor the process of wound healing. After that, HA-KPV-NPs with various KPV concentrations were added to the wells.

In Vitro Anti-inflammation Test

Raw 264.7 macrophages were seeded in six-well plates at a density of 1×10^5 cells/well and incubated overnight. After co-culture with various NPs for 5 hr, cells were incubated in medium containing 10% FBS for 19, 43, 67, or 91 hr. Raw 264.7 macrophages were then stimulated with LPS (1 μg/mL, Sigma) for 3 hr. Total RNA was extracted using RNeasy Plus Mini Kit (Qiagen). The cDNA was generated from the total RNAs isolated above using the Maxima first strand cDNA synthesis kit (Fermentas) according to the manufacturer's instruction. TNF-α mRNA expression levels were quantified by qRT-PCR using Maxima SYBR Green/ROX qPCR Master Mix (Fermentas). The data were normalized to the internal control: 36B4. Relative gene expression levels were calculated using the $2^{-\Delta\Delta Ct}$ method. Sequences of all the primers used for qRT-PCR are given in Table S1.

Induction of UC Mouse Model and Oral Administration of NPs

FVB male mice (8 weeks of age, The Jackson Laboratory) were used in the animal experiments. Mice were group housed (25°C), photoperiod (12:12 h light-dark cycle), and allowed unrestricted access to potables and standard mouse chow. All the animal experiments were approved by Georgia State University Institutional Animal Care and Use Committee.

To track the HA-functionalized NPs in GIT after oral administration, the near infrared dye DiR was employed as a fluorescence probe. Colitis was induced in FVB male mice by replacing their drinking water with a 3.5% (wt/vol) DSS (36–50 kDa). DiR-loaded NP-embedded

hydrogel was orally administered to mice at an equivalent DiR concentration (0.5 mg DiR/kg per mouse) after 6 days of DSS treatment. After oral administration for 4, 18, and 24 hr, respectively, the mice were sacrificed to obtain GIT. The images were captured using the IVIS spectrum imaging system (PerkinElmer/Caliper LifeSciences).

Colitis was induced in FVB male mice (8 weeks of age, The Jackson Laboratory) by replacing their drinking water with a 3.5% (wt/vol) DSS (36–50 kDa) for 6 days. To investigate the in vivo targeting property of NPs, mice were orally administered with CM-loaded NP-embedded hydrogel (5 mg CM/kg per mouse). After 12 hr, the mice were euthanized. Then spleen and colon were removed. Isolation of splenocytes and lamina propria immune cells was conducted as described in previous reports.[54,55] Antibodies used for analysis were from eBioscience unless otherwise noted: anti-mouse CD11b eFluor 450, anti-mouse F4/80 antigen PE-Cy7, anti-mouse CD4 eFluor 450 and anti-mouse CD4 PE-Cy7 (BD Pharmingen). Flow cytometric analysis was performed on a BD LSRFortessa flow cytometer (BD Biosciences), and data were analyzed using the FlowJo v10 processing program.

UC was induced by replacing the drinking water of the mice with a 3% (wt/vol) DSS solution for 8 days. To deliver various NPs to mice colonic lumen, we encapsulated them into a hydrogel comprised of chitosan and alginate and double-gavaged the mice for 5 days. Mice receiving NPs were treated with 16 μg/kg of KPV per day. Control mice were given water only. Mice were observed daily and evaluated for changes in body weight and development of clinical symptoms of colitis. Mice were sacrificed by CO_2 euthanasia. Spleen weight and colon length were measured. A small piece (50 mg) of distal colon was taken for MPO and RNA analysis, and the remaining of the colon was used for histopathological analysis.

Ex Vivo Cellular Uptake of NPs

Colitis was induced in FVB male mice (8 weeks of age, The Jackson Laboratory) by replacing their drinking water with a 3.5% (wt/vol) DSS (36–50 kDa) for 6 days. Colitis tissues (6−8 mm) from DSS-treated mice were placed in 24-well culture plates with the mucosal surface facing upward. The wells were flooded in serum-free RPMI-1640 medium, and then HA-CM-NPs suspensions (CM, 100 μM) were added to each well. After 5 hr of co-incubation, tissues were washed thoroughly with PBS for 3 times and then embedded in OCT. Sections (5 μm) were fixed in 4% paraformaldehyde and further stained with DAPI. Images were acquired using an Olympus microscope equipped with a Hamamatsu Digital Camera ORCA-03G.

MPO Activity

Neutrophil infiltration into the colon was quantified by measuring the MPO activity. Briefly, a portion of colon was homogenized in 1:20 (w/v) of 50 mM phosphate buffer (pH 6.0) containing 0.5% hexadecyltrimethyl ammonium bromide (Sigma) on ice using a homogenizer (Polytron). The homogenate was then sonicated for 10 s, freeze-thawed three times, and centrifuged at 16,000 × *g* for 15 min. The supernatant was then added to 1 mg/mL *O*-dianisidine hydrochloride (Sigma) and 0.0005% hydrogen peroxide, and the change in absorbance at 460 nm was measured. MPO activity was expressed as units per gram of colonic tissue, where one unit was defined as the amount that degrades 1 μmol of hydrogen peroxide per min at 25°C.

H&E Staining

Tissue samples were evaluated for mucosal architecture change, cellular infiltration, inflammation, goblet cell depletion, surface epithelial cell hyperplasia, and signs of epithelial regeneration using light microscopy of H&E staining. These values were used to assess the degrees of mucosal damage and repair in various groups. Colon tissues were fixed in 10% buffered formalin (Fisher) and embedded in paraffin. Tissue sections with a thickness of 5 μm were stained with H&E followed by imaging using bright-field microscopy.

In Vivo TNF-α mRNA Expression Level

Total RNA was extracted from the tissue samples using RNeasy Plus Mini Kit (Qiagen). The cDNA was generated from the total RNAs isolated above using the Maxima first strand cDNA synthesis kit (Fermentas) according to the manufacturer's instruction. The mRNA expression levels of TNF-α were quantified by real-time RT-PCR using Maxima SYBR Green/ROX qPCR Master Mix (Fermentas).

Statistical Analysis

Statistical analysis was performed using ANOVA followed by a Bonferroni post hoc test (GraphPad Prism) or Student's t test. Data are expressed as mean ± SEM. Statistical significance is represented by $^{*}p < 0.05$ and $^{**}p < 0.01$.

SUPPLEMENTAL INFORMATION

Supplemental Information includes three figures and one table and can be found with this article online at http://dx.doi.org/10.1016/j.ymthe.2016.11.020.

AUTHOR CONTRIBUTIONS

B.X. and D.M. conceived and deigned the experiments, analyzed the data, and wrote the manuscript. B.X., Z.X., E.V., Y.Z., Z.Z., M.Z., and Y.K. performed the experiments.

CONFLICTS OF INTEREST

The authors declare no conflicts of interest.

ACKNOWLEDGMENTS

This work was supported by grants from the Department of Veterans Affairs (BX002526), the National Institutes of Health of Diabetes and Digestive and Kidney (RO1-DK-071594), the National Natural Science Foundation of China (51503172 and 81571807), the Fundamental Research Funds for the Central Universities (SWU114086 and XDJK2015C067), the Basic and Frontier Research Project of Chongqing (cstc2016jcyjA0078) and the Scientific Research Foundation for the Returned Overseas Chinese Scholars (State Education Ministry). D.M. is a recipient of a Career Scientist Award from the Department of Veterans Affairs.

REFERENCES

1. Patel, M.M. (2016). Micro/nano-particulate drug delivery systems: a boon for the treatment of inflammatory bowel disease. Expert Opin. Drug Deliv. *13*, 771–775.
2. Frede, A., Neuhaus, B., Klopfleisch, R., Walker, C., Buer, J., Müller, W., Epple, M., and Westendorf, A.M. (2016). Colonic gene silencing using siRNA-loaded calcium phosphate/PLGA nanoparticles ameliorates intestinal inflammation in vivo. J. Control. Release *222*, 86–96.
3. Pineton de Chambrun, G., Peyrin-Biroulet, L., Lemann, M., and Colombel, J.F. (2010). Clinical implications of mucosal healing for the management of IBD. Nat. Rev. Gastroenterol. Hepatol. *7*, 15–29.
4. Iacucci, M., de Silva, S., and Ghosh, S. (2010). Mesalazine in inflammatory bowel disease: a trendy topic once again? Can. J. Gastroenterol. *24*, 127–133.
5. Lautenschläger, C., Schmidt, C., Fischer, D., and Stallmach, A. (2014). Drug delivery strategies in the therapy of inflammatory bowel disease. Adv. Drug Deliv. Rev. *71*, 58–76.
6. Xiao, B., Laroui, H., Ayyadurai, S., Viennois, E., Charania, M.A., Zhang, Y., and Merlin, D. (2013). Mannosylated bioreducible nanoparticle-mediated macrophage-specific TNF-α RNA interference for IBD therapy. Biomaterials *34*, 7471–7482.
7. Lamprecht, A. (2003). Multiparticulate systems in the treatment of inflammatory bowel disease. Curr. Drug Targets Inflamm. Allergy *2*, 137–144.
8. Brzoska, T., Luger, T.A., Maaser, C., Abels, C., and Böhm, M. (2008). Alpha-melanocyte-stimulating hormone and related tripeptides: biochemistry, antiinflammatory and protective effects in vitro and in vivo, and future perspectives for the treatment of immune-mediated inflammatory diseases. Endocr. Rev. *29*, 581–602.
9. Kannengiesser, K., Maaser, C., Heidemann, J., Luegering, A., Ross, M., Brzoska, T., Bohm, M., Luger, T.A., Domschke, W., and Kucharzik, T. (2008). Melanocortin-derived tripeptide KPV has anti-inflammatory potential in murine models of inflammatory bowel disease. Inflamm. Bowel Dis. *14*, 324–331.
10. Luger, T.A., Scholzen, T.E., Brzoska, T., and Böhm, M. (2003). New insights into the functions of alpha-MSH and related peptides in the immune system. Ann. N Y Acad. Sci. *994*, 133–140.
11. Laroui, H., Dalmasso, G., Nguyen, H.T., Yan, Y., Sitaraman, S.V., and Merlin, D. (2010). Drug-loaded nanoparticles targeted to the colon with polysaccharide hydrogel reduce colitis in a mouse model. Gastroenterology *138*, 843–853.
12. Dalmasso, G., Charrier-Hisamuddin, L., Nguyen, H.T., Yan, Y., Sitaraman, S., and Merlin, D. (2008). PepT1-mediated tripeptide KPV uptake reduces intestinal inflammation. Gastroenterology *134*, 166–178.
13. Xiao, B., Laroui, H., Viennois, E., Ayyadurai, S., Charania, M.A., Zhang, Y., Zhang, Z., Baker, M.T., Zhang, B., Gewirtz, A.T., and Merlin, D. (2014). Nanoparticles with surface antibody against CD98 and carrying CD98 small interfering RNA reduce colitis in mice. Gastroenterology *146*, 1289–1300.
14. Laroui, H., Viennois, E., Xiao, B., Canup, B.S., Geem, D., Denning, T.L., and Merlin, D. (2014). Fab'-bearing siRNA TNFα-loaded nanoparticles targeted to colonic macrophages offer an effective therapy for experimental colitis. J. Control. Release *186*, 41–53.
15. Laroui, H., Geem, D., Xiao, B., Viennois, E., Rakhya, P., Denning, T., and Merlin, D. (2014). Targeting intestinal inflammation with CD98 siRNA/PEI-loaded nanoparticles. Mol. Ther. *22*, 69–80.
16. Laroui, H., Theiss, A.L., Yan, Y., Dalmasso, G., Nguyen, H.T., Sitaraman, S.V., and Merlin, D. (2011). Functional TNFα gene silencing mediated by polyethyleneimine/TNFα siRNA nanocomplexes in inflamed colon. Biomaterials *32*, 1218–1228.
17. Knipe, J.M., Strong, L.E., and Peppas, N.A. (2016). Enzyme- and pH-responsive microencapsulated nanogels for oral delivery of siRNA to induce TNF-α knockdown in the intestine. Biomacromolecules *17*, 788–797.
18. Xiao, B., and Merlin, D. (2012). Oral colon-specific therapeutic approaches toward treatment of inflammatory bowel disease. Expert Opin. Drug Deliv. *9*, 1393–1407.
19. Xiao, B., Yang, Y., Viennois, E., Zhang, Y., Ayyadurai, S., Baker, M., Laroui, H., and Merlin, D. (2014). Glycoprotein CD98 as a receptor for colitis-targeted delivery of nanoparticle. J. Mater. Chem. B Mater. Biol. Med. *2*, 1499–1508.
20. Fromont Hankard, G., Cezard, J.P., Aigrain, Y., Navarro, J., and Peuchmaur, M. (1998). CD44 variant expression in inflammatory colonic mucosa is not disease specific but associated with increased crypt cell proliferation. Histopathology *32*, 317–321.
21. Farkas, S., Hornung, M., Sattler, C., Anthuber, M., Gunthert, U., Herfarth, H., Schlitt, H.J., Geissler, E.K., and Wittig, B.M. (2005). Short-term treatment with anti-CD44v7 antibody, but not CD44v4, restores the gut mucosa in established chronic dextran sulphate sodium (DSS)-induced colitis in mice. Clin. Exp. Immunol. *142*, 260–267.
22. Dreaden, E.C., Morton, S.W., Shopsowitz, K.E., Choi, J.H., Deng, Z.J., Cho, N.J., and Hammond, P.T. (2014). Bimodal tumor-targeting from microenvironment responsive hyaluronan layer-by-layer (LbL) nanoparticles. ACS Nano *8*, 8374–8382.
23. Xiao, B., Han, M.K., Viennois, E., Wang, L., Zhang, M., Si, X., and Merlin, D. (2015). Hyaluronic acid-functionalized polymeric nanoparticles for colon cancer-targeted combination chemotherapy. Nanoscale *7*, 17745–17755.
24. Almeida, P.V., Shahbazi, M.A., Mäkilä, E., Kaasalainen, M., Salonen, J., Hirvonen, J., and Santos, H.A. (2014). Amine-modified hyaluronic acid-functionalized porous silicon nanoparticles for targeting breast cancer tumors. Nanoscale *6*, 10377–10387.
25. Lo, C.T., Van Tassel, P.R., and Saltzman, W.M. (2010). Poly(lactide-co-glycolide) nanoparticle assembly for highly efficient delivery of potent therapeutic agents from medical devices. Biomaterials *31*, 3631–3642.
26. Steinbach, J.M., Weller, C.E., Booth, C.J., and Saltzman, W.M. (2012). Polymer nanoparticles encapsulating siRNA for treatment of HSV-2 genital infection. J. Control. Release *162*, 102–110.
27. Fonte, P., Lino, P.R., Seabra, V., Almeida, A.J., Reis, S., and Sarmento, B. (2016). Annealing as a tool for the optimization of lyophilization and ensuring of the stability of protein-loaded PLGA nanoparticles. Int. J. Pharm. *503*, 163–173.
28. Cohen-Sela, E., Chorny, M., Koroukhov, N., Danenberg, H.D., and Golomb, G. (2009). A new double emulsion solvent diffusion technique for encapsulating hydrophilic molecules in PLGA nanoparticles. J. Control. Release *133*, 90–95.
29. Mora-Huertas, C.E., Fessi, H., and Elaissari, A. (2011). Influence of process and formulation parameters on the formation of submicron particles by solvent displacement and emulsification-diffusion methods critical comparison. Adv. Colloid Interface Sci. *163*, 90–122.
30. Hassan, C.M., and Peppas, N.A. (2000). Structure and applications of poly(vinyl alcohol) hydrogels produced by conventional crosslinking or by freezing/thawing methods. Adv. Polym. Sci. *153*, 37–65.
31. Mu, L., and Feng, S.S. (2003). PLGA/TPGS nanoparticles for controlled release of paclitaxel: effects of the emulsifier and drug loading ratio. Pharm. Res. *20*, 1864–1872.
32. Xiao, B., Si, X., Han, M.K., Viennois, E., Zhang, M., and Merlin, D. (2015). Co-delivery of camptothecin and curcumin by cationic polymeric nanoparticles for synergistic colon cancer combination chemotherapy. J. Mater. Chem. B Mater. Biol. Med. *3*, 7724–7733.
33. Xiao, B., Zhang, M., Viennois, E., Zhang, Y., Wei, N., Baker, M.T., Jung, Y., and Merlin, D. (2015). Inhibition of MDR1 gene expression and enhancing cellular uptake for effective colon cancer treatment using dual-surface-functionalized nanoparticles. Biomaterials *48*, 147–160.
34. Kim, T.H., Ihm, J.E., Choi, Y.J., Nah, J.W., and Cho, C.S. (2003). Efficient gene delivery by urocanic acid-modified chitosan. J. Control. Release *93*, 389–402.
35. Liu, Y., and Reineke, T.M. (2005). Hydroxyl stereochemistry and amine number within poly(glycoamidoamine)s affect intracellular DNA delivery. J. Am. Chem. Soc. *127*, 3004–3015.
36. Zhang, S., Ermann, J., Succi, M.D., Zhou, A., Hamilton, M.J., Cao, B., Korzenik, J.R., Glickman, J.N., Vemula, P.K., Glimcher, L.H., et al. (2015). An inflammation-targeting hydrogel for local drug delivery in inflammatory bowel disease. Sci. Transl. Med. *7*, 300ra128.
37. Oueslati, N., Leblanc, P., Harscoat-Schiavo, C., Rondags, E., Meunier, S., Kapel, R., and Marc, I. (2014). CTAB turbidimetric method for assaying hyaluronic acid in complex environments and under cross-linked form. Carbohydr. Polym. *112*, 102–108.
38. Singh, S.P., Sharma, M., and Gupta, P.K. (2015). Cytotoxicity of curcumin silica nanoparticle complexes conjugated with hyaluronic acid on colon cancer cells. Int. J. Biol. Macromol. *74*, 162–170.
39. Perše, M., and Cerar, A. (2012). Dextran sodium sulphate colitis mouse model: traps and tricks. J. Biomed. Biotechnol. *2012*, 718617.

40. Grisham, M.B. (2008). Do different animal models of IBD serve different purposes? Inflamm. Bowel Dis. *14* (*Suppl 2*), S132–S133.

41. Theiss, A.L., Laroui, H., Obertone, T.S., Chowdhury, I., Thompson, W.E., Merlin, D., and Sitaraman, S.V. (2011). Nanoparticle-based therapeutic delivery of prohibitin to the colonic epithelial cells ameliorates acute murine colitis. Inflamm. Bowel Dis. *17*, 1163–1176.

42. van Furth, R., Cohn, Z.A., Hirsch, J.G., Humphrey, J.H., Spector, W.G., and Langevoort, H.L. (1972). The mononuclear phagocyte system: a new classification of macrophages, monocytes, and their precursor cells. Bull. World Health Organ. *46*, 845–852.

43. Grimm, M.C., Pullman, W.E., Bennett, G.M., Sullivan, P.J., Pavli, P., and Doe, W.F. (1995). Direct evidence of monocyte recruitment to inflammatory bowel disease mucosa. J. Gastroenterol. Hepatol. *10*, 387–395.

44. Platt, A.M., Bain, C.C., Bordon, Y., Sester, D.P., and Mowat, A.M. (2010). An independent subset of TLR expressing CCR2-dependent macrophages promotes colonic inflammation. J. Immunol. *184*, 6843–6854.

45. Bain, C.C., Bravo-Blas, A., Scott, C.L., Gomez Perdiguero, E., Geissmann, F., Henri, S., Malissen, B., Osborne, L.C., Artis, D., and Mowat, A.M. (2014). Constant replenishment from circulating monocytes maintains the macrophage pool in the intestine of adult mice. Nat. Immunol. *15*, 929–937.

46. Cheng, C.J., Tietjen, G.T., Saucier-Sawyer, J.K., and Saltzman, W.M. (2015). A holistic approach to targeting disease with polymeric nanoparticles. Nat. Rev. Drug Discov. *14*, 239–247.

47. Laroui, H., Wilson, D.S., Dalmasso, G., Salaita, K., Murthy, N., Sitaraman, S.V., and Merlin, D. (2011). Nanomedicine in GI. Am. J. Physiol. Gastrointest. Liver Physiol. *300*, G371–G383.

48. Lamprecht, A., Ubrich, N., Yamamoto, H., Schäfer, U., Takeuchi, H., Maincent, P., Kawashima, Y., and Lehr, C.M. (2001). Biodegradable nanoparticles for targeted drug delivery in treatment of inflammatory bowel disease. J. Pharmacol. Exp. Ther. *299*, 775–781.

49. Jubeh, T.T., Barenholz, Y., and Rubinstein, A. (2004). Differential adhesion of normal and inflamed rat colonic mucosa by charged liposomes. Pharm. Res. *21*, 447–453.

50. Lavertu, M., Méthot, S., Tran-Khanh, N., and Buschmann, M.D. (2006). High efficiency gene transfer using chitosan/DNA nanoparticles with specific combinations of molecular weight and degree of deacetylation. Biomaterials *27*, 4815–4824.

51. Badawy, M.E.I., and Rabea, E.I. (2009). Potential of the biopolymer chitosan with different molecular weights to control postharvest gray mold of tomato fruit. Postharvest Biol. Technol. *51*, 110–117.

52. Bhatnagar, P., Pant, A.B., Shukla, Y., Panda, A., and Gupta, K.C. (2016). Hyaluronic acid grafted PLGA copolymer nanoparticles enhance the targeted delivery of Bromelain in Ehrlich's Ascites Carcinoma. Eur. J. Pharm. Biopharm. *105*, 176–192.

53. Vangara, K.K., Liu, J.L., and Palakurthi, S. (2013). Hyaluronic acid-decorated PLGA-PEG nanoparticles for targeted delivery of SN-38 to ovarian cancer. Anticancer Res. *33*, 2425–2434.

54. Denning, T.L., Wang, Y.C., Patel, S.R., Williams, I.R., and Pulendran, B. (2007). Lamina propria macrophages and dendritic cells differentially induce regulatory and interleukin 17-producing T cell responses. Nat. Immunol. *8*, 1086–1094.

55. Denning, T.L., Norris, B.A., Medina-Contreras, O., Manicassamy, S., Geem, D., Madan, R., Karp, C.L., and Pulendran, B. (2011). Functional specializations of intestinal dendritic cell and macrophage subsets that control Th17 and regulatory T cell responses are dependent on the T cell/APC ratio, source of mouse strain, and regional localization. J. Immunol. *187*, 733–747.